Indian Journal of Biochemistry & Biophysics
Vol. 59, September 2022, pp. 892-899
DOI: 10.56042/ijbb.v59i9.59916

Effective adsorption of drug from aqueous solution using citric acid functionalized magnetite nanoparticles and their antibacterial studies

Arti Jangra, Jaiveer Singh, Jai Kumar, Keerti Rani & Ramesh Kumar*
Department of Chemistry, Kurukshetra University, Kurukshetra-136 119, Haryana, India

Received 01 February 2022; *revised 25 August 2022*

The synthesis of magnetite nanoparticles and their applications after surface modification have drawn in the eye of researchers toward it all through the previous a few times. In the present study, the synthesis of citric acid-modified magnetic nanoparticles has been reported. Numerous technical approaches such as x-ray diffraction, field emission scanning electron microscopy, thermogravimetric analysis and fourier transform infrared spectroscopy were accustomed to characterize these synthesized magnetite nanoparticles. The main emphasis of this examination was to study the adsorption behavior of these synthesized nanoparticles for ciprofloxacin drug from aqueous solution. The influences of various experimental parameters including pH, the contact time, amount of nanoparticles and initial concentration of ciprofloxacin drug, were investigated simultaneously. Moreover, isotherm study was observed to follow Langmuir isotherm model and the value of maximum adsorption capacity was 20.65 mg/g as calculated. Furthermore, the kinetic study was found to fit well with pseudo-second-order kinetics model. The overall study suggested that these functionalized magnetite nanoparticles can be utilized as a proficient tool for the adsorption of drug from aqueous solution. The antibacterial behavior of these drug loaded nanoparticles was also scrutinized.

Keywords: Adsorption process, Antibacterial activity, Ciprofloxacin, Citric acid, Magnetite nanoparticles

Pharmaceuticals attract global attention toward themselves because these are referred as prominent environmental pollutants. The residues of pharmaceuticals are highly toxic. These are also found in ground and surface water and can be easily taken up by human bodies. Antibiotics, a class of pharmaceuticals, have received priority because of their extensive use in human and animal health. Their presence in the environment harms human and aquatic life. So, the treatment of wastewater became a necessity. Among various antibiotics, quinolone antibiotics were used commonly. Ciprofloxacin (CIP) is a second-generation quinolone that can be used for living creatures. CIP is found to be present in a larger extent in contaminated water than other antibiotics[1]. The most appropriate methods which are used for the exclusion of ciprofloxacin drug from wastewater are adsorption[2], chemical oxidation[3] and photolytic reduction[4], *etc*. Among these, the adsorption process is considered as the most effective and efficient method for the removal of CIP. Numerous researchers have used various adsorbents for this purpose, such as Li *et al.* used kaolinite for CIP removal and observed their adsorption capacity[5] Jiang *et al.* used birnessite[6], while Rakshit *et al.* used nano-sized magnetite[7] for the removal of CIP drug. Wang *et al.* used magnetic chitosan grafted graphene oxide[8] and Ngo *et al.* used bamboo-based activated carbon to achieve high adsorption capacities[9]. Khoshnamvand *et al.* used magnesium oxide nanoparticles[10], whereas, Li *et al.* used bio-char obtained from tea leaves to adsorb CIP from aqueous solution[11]. In the last few decades, nanoparticles emerged as an excellent candidate because of their large surface to volume ratio. Among different types of nano-sized magnetic particles, superparamagnetic iron oxide nanoparticles have great potential in various fields such as environmental and biomedical, due to their biocompatibility and high chemical stability compared to various metallic iron oxide nanoparticles[12,13]. Numerous methods have been used to prepare iron oxide nanoparticles such as co-precipitation, sol-gel and hydrothermal, *etc*. Magnetite nanoparticles are commonly used. Moreover, surface modification of magnetic nanoparticles by different coating materials like humic acid, chitosan *etc*., have been attracted very much attention of researchers towards itself due to their unique properties such as easy separation under external magnetic field and fast adsorption kinetics. Coating material having different functional groups such as

*Correspondence:
E-mail: rameshkumarkuk@gmail.com

carboxylate, sulfur and phosphate is known to bind with the surface of magnetic nanoparticles, thus provides stability to modified nanoparticles and also prevent them from agglomeration. Thus, the interaction between the coating material and magnetic nanoparticles is crucial from the application point of view. The small coating molecules are mainly attractive due to their easy synthesis and chemistry[14,15].

The aim of the present work is to synthesize citric acid-coated magnetic nanoparticles further used as an effective adsorbent to adsorb CIP drug from aqueous solutions.

Materials and Methods

Materials

Ferrous sulfateheptahydrate ($FeSO_4.7H_2O$, 98%), ferric chloride hexahydrate ($FeCl_3.6H_2O$, 97%), ammonium hydroxide solution (25%), ciprofloxacin and citric acid were purchased from SRL (India) and used without any further purification.

Instruments

The infrared spectra of pure citric acid (CA), bare magnetite nanoparticles (Fe_3O_4) and CA coated magnetite nanoparticles (CA@ Fe_3O_4) were recorded using the MB-3000 ABB FTIR spectrometer. Absorbance measurements were obtained using a T90 PG Instrument Limited UV-visible spectrophotometer (900-190 nm). The thermal analysis of nanoparticles was performed by Perkin Elmer STA-6000 thermogravimetric analyzer (heating rate 5-80°C/min and the temperature range 20-1000°C). The average size of nanoparticles was monitored using the Hitachi SU-8000 field emission scanning electron microscope (FESEM) and particle size analyzer (Microtrac W3602). An instrument employing Cu Kα radiation (λ=1.540 A°) was used to record X-ray diffraction (XRD) patterns at room temperature. A digital mechanical stirrer (2000 rpm) was used to synthesize magnetic nanoparticles.

Synthesis of magnetic nanoparticles and their surface modification

The method for the preparation of magnetic nanoparticles was based on the co-precipitation method. Typically, 6.1 g of $FeCl_3.6H_2O$ was dissolved in 100 mL of de-ionized water with 4.2 g of $FeSO_4.7H_2O$. The solution was heated up to 90°C, followed by the rapid addition of 10 mL of NH_4OH (25%). The black-colored uncoated iron oxide nanoparticles were precipitated[16]. The 10 mL solution of citric acid (0.5 g/mL) was added for surface modification of uncoated magnetic nanoparticles and stirred for another 30 min[17]. Then these coated magnetic nanoparticles were separated from the solution using the decantation method by applying an external magnetic field.

Batch adsorption experiments:

Citric acid coated magnetite nanoparticles were used as adsorbents for the adsorption of CIP drug from aqueous solutions. Adsorption experiments were performed at room temperature using batch adsorption processes. The effect of various parameters such as pH of the solution (2 to 9), the amount of citric acid coated magnetite nanoparticles (5-30 mg), contact time (0-120 min) and CIP drug concentration (10-50 ppm) on CIP adsorption were investigated[10]. The equilibrium time was determined using the fixed concentration of CIP drug and adsorbent. Further, the effect of variation in the initial CIP drug concentration solution also studied at equilibrium time using variable amount of adsorbent (5 to 30 mg).

The adsorption capacity (q_e) was calculated using the formula:

$$qe = \frac{(C_0 - C_e)V}{m}$$

The percentage removal of CIP drug was determined using the equation:

$$\% R = \frac{(C_0 - C_e)}{C_0} X\ 100$$

Adsorption effect on initial and final concentrations of CIP drug was measured by recording the absorbance at 275 nm using a UV-Visible spectrophotometer.

Several isotherm (Table 1) and kinetic (Table 2) models such as Langmuir[18,19], Freundlich[20,21], Temkin[22,23] and Pseudo first-order[24,25], as well as second-order[26,27] kinetic equations, were studied to evaluate the behavior and adsorption rate of CIP drug onto the

Table 1— Equations of Isotherms

Isotherm Model	Equations
Langmuir	$q_e = \frac{q_m b C_e}{1 + bC_e}$
Freundlich	$q_e = K_f . C_e^{1/n}$
Temkin	$q_e = B\ln A + B\ \ln C_e$ Where, $B = \frac{RT}{b}$

Table 2— Equations of Kinetics

Kinetic Model	Equations
Pseudo-First-Order	$\log(q_e - q_t) = \log q_e - \frac{k_1 t}{2.303}$
Pseudo-second-Order	$\frac{t}{q_t} = \frac{1}{k_2 q_e^2} + \frac{t}{q_e}$

surface of CA coated magnetic nanoparticles, respectively.

Antibacterial Studies of CIP drug and CIP drug adsorbed citric acid coated magnetite nanoparticles (CIP@CA@Fe_3O_4)

Agar well diffusion method was employed to scrutinize the antibacterial behavior[28] of drug loaded citric acid coated magnetite nanoparticles (CIP@CA@Fe3O4) against various gram positive (*Bacillus subtilis* and *Staphylococcus aureus*) and gram negative (*Pseudomonas aeruginosa* and *Escherichia coli*) bacterial strains. Petriplates containing 20 mL Muller Hinton medium were seeded with 24 h culture of bacterial strains. Wells were cut and 20 µL of the given compound extracts were added. The plates were then incubated at 37°C for 24 h. The antibacterial activity was assayed by measuring the diameter of the inhibition zone formed around the well.

Results and Discussion

Characterization of bare (Fe_3O_4) and surface modified nanoparticles (CA@Fe_3O_4)

Both bare magnetite nanoparticles, Fe_3O_4 and citric acid coated magnetite nanoparticles, CA@Fe_3O_4 were dispersed in water using Analab, India ultrasonicator (15 kHz, 300 W) to determine their average size and size distribution.

Fourier transform infrared spectral studies

The fourier transform spectra of prepared bare magnetite nanoparticles (Fe_3O_4), pure citric acid and citric acid coated magnetite nanoparticles (CA@Fe_3O_4) were recorded within range 500-4000 cm^{-1}. Fourier transform infrared (FTIR) spectrum of Fe_3O_4 showed peaks near 600 cm^{-1} that corresponds to Fe-O stretching vibration and band at 3300 cm^{-1} might be assigned to –OH stretching. Infrared (IR) of pure citric acid and citric acid coated magnetite nanoparticles depicts a representative peak for C=O stretching near 1700 cm^{-1} (Fig. 1), which demonstrates the binding of citric acid to Fe_3O_4 nanoparticles by chemisorptions of citrate ions[29]. Two new peaks at 1625 cm^{-1} and

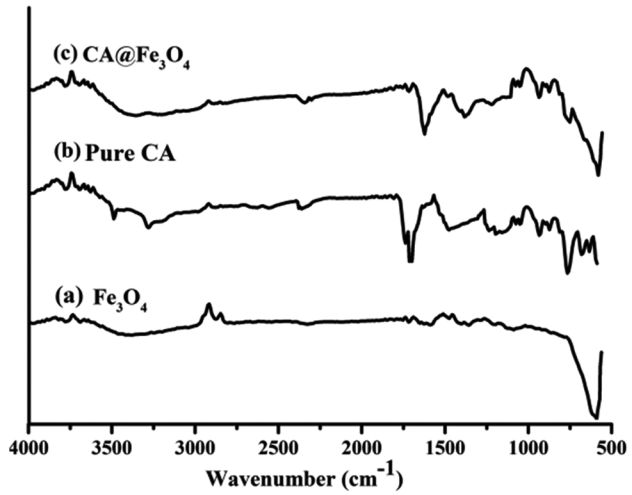

Fig. 1 — Fourier transform infrared spectra of pure citric acid (Pure CA), bare magnetite nanoparticles (Fe_3O_4) and citric acid functionalized magnetite nanoparticles (CA@Fe_3O_4)

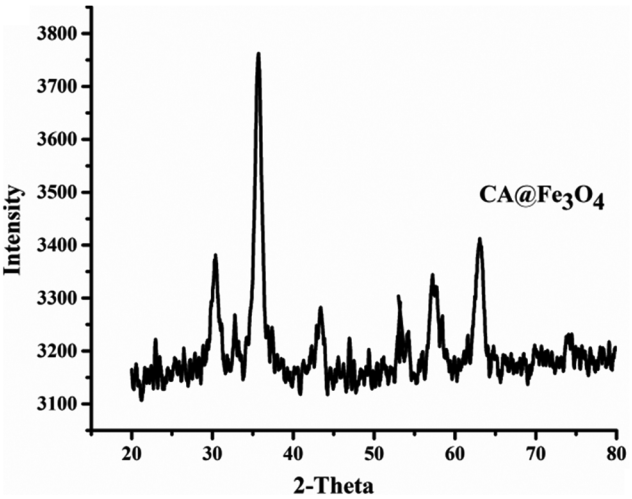

Fig. 2 — X-ray diffraction pattern of citric acid functionalized magnetite nanoparticles (CA@Fe_3O_4)

1427 cm^{-1} may be assigned to asymmetric and symmetric stretching of carboxylate group. Thus, the presence of these peaks confirmed the coating of citric acid on the surface of Fe_3O_4 as these new peaks resemble the peaks present in the IR spectrum of pure citric acid and bare magnetite nanoparticles, Fe_3O_4.

X-ray diffraction

X-ray diffraction pattern (XRD) of CA@Fe_3O_4 nanoparticles was recorded in 2θ range of 20º-80º (Fig. 2) and the mean size of nanoparticles was theoretically calculated from XRD peaks, using the Debye-Scherrer equation:

$$d = (0.914\lambda / \beta \cos\theta)$$

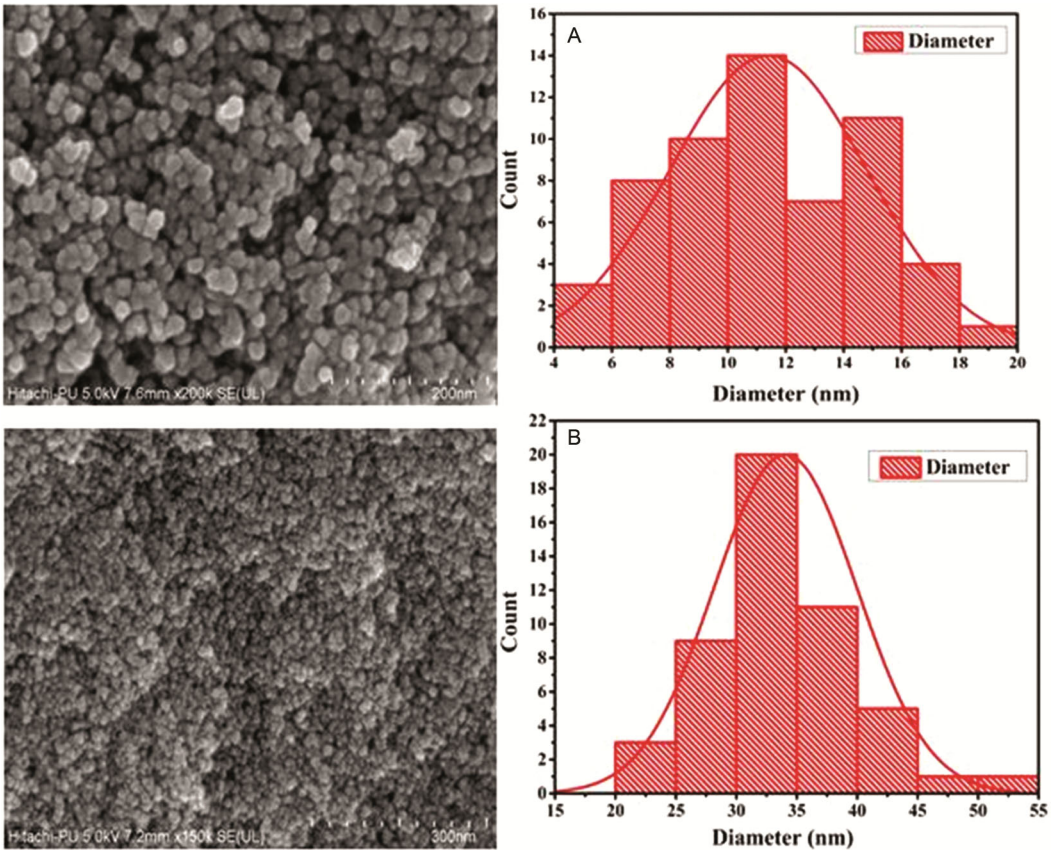

Fig. 3 — Field emission scanning electron microscope images and histogram curves of bare magnetite nanoparticles (Fe_3O_4) (A) [1 division= 20 nm] and citric acid functionalized magnetite nanoparticles ($CA@Fe_3O_4$) (B) [1 division= 30 nm]

Where, $\lambda$is the ray wavelength (1.540 A°), βfull-width at half maximum and θ is Bragg angle in degree. The XRD pattern of $CA@Fe_3O_4$ nanoparticles depicted five crystalline peaks, which suggest their semi-crystalline nature. The average diameter calculated for $CA@Fe_3O_4$ magnetic nanoparticles was 32.5 nm. These results are close to the results shown by field emission scanning electron microscope studies.

Field emission scanning electron microscopy

Field emission scanning electron microscope (FESEM) images depict the particle size of prepared Fe_3O_4 and $CA@Fe_3O_4$ magnetic nanoparticles and the average size was found to be 11 nm and 34 nm, respectively (Fig. 3). The increase in the size of bare magnetite nanoparticles, Fe_3O_4 after coating suggested the successful coating of citric acid on the surface of bare magnetite nanoparticles, Fe_3O_4.

Thermogravimetric analysis

The thermal behavior of magnetic nanoparticles before and after coating was analyzed under atmospheric conditions using thermogravimetric analysis (TGA) technique. Thermo grams display two thermal stages for bare magnetic nanoparticles and three stages for citric acid-coated magnetite nanoparticles. The weight loss at first stage for both took place within the region 10-150°C, which might be due to the loss of hydroxyl

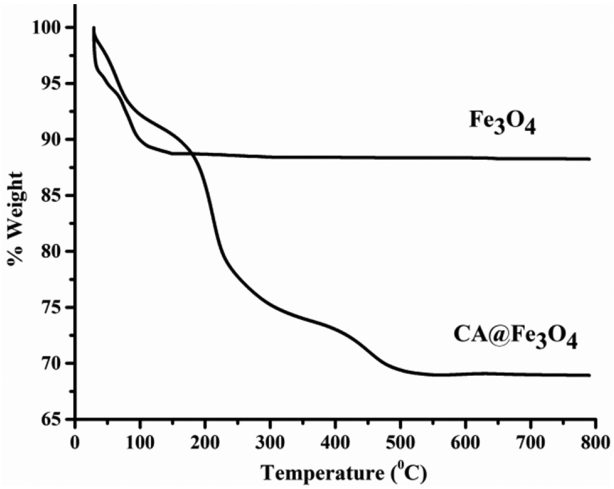

Fig. 4 — Thermogravimetric curves for bare magnetite nanoparticles (Fe_3O_4) and citric acid functionalized magnetite nanoparticles ($CA@Fe_3O_4$)

groups, *i.e.*, water molecules. Besides, a considerable weight loss was indicated after 220°C for citric coated magnetite nanoparticles (Fig. 4), which could be attributed to the thermal degradation of the citric acid coating. The temperature range was higher than that for the pure citric acid resulting that the magnetic nanoparticles enhanced the thermal stability of citric acid[30]. The third stage of weight loss was observed beyond 400°C, which probably related to iron oxide nanoparticles. Thus, the comparison of the thermograms resulted that the net weight loss for Fe_3O_4 and CA@ Fe_3O_4 was found to be 11.76% and 31.05%, respectively.

Adsorption studies of CA@Fe_3O_4 with variation in different parameters

Batch adsorption experiments were performed to examine the effects of various adsorption parameters such as the pH, contact time, CIP drug concentration (varying from 10 to 50 ppm) and amount of adsorbent (CA@Fe_3O_4), on the adsorption behavior of CA@Fe_3O_4.

Effect of pH

Drug adsorption capacity of nanoparticles can be prejudiced by the changing the surface charge density of nanoparticles. The variation of pH on the adsorption of drug can be inspected in the pH range of 2-9 value with different initial concentration of adsorbate and fixed amount of adsorbent (30 mg). The adsorption capacity gradually rises on increasing the pH of solution ranging from 2-7 and starts declining from 7-9 (Fig. 5). This growing effect may be accredited due to the electrostatic interactions between the adsorbate (possess cationic nature) and adsorbent. When the adsorption system reaches equilibrium, the pH of solution does not have any influence on the adsorption capacity[31]. At pH greater than 7, the drug solution is charged negatively, and citric acid magnetite nanoparticles are charged negatively. Therefore, repulsion forces occur and the adsorption capacities decreases[32].

Effect of time

The influence of prepared citric acid coated magnetite nanoparticles regarding about the removal of drug from aqueous solution was studied as a function of time using batch adsorption methods at pH 7, fixed concentration of drug solution (50 ppm) and different amount of citric acid coated magnetite nanoparticles (05-30 mg) at room temperature and 2000 rpm stirring rate. The percentage removal efficiency of coated magnetite nanoparticles displays parallel performance for variable amount of adsorbent *i.e.* rises progressively at primary stage with contact time and achieves a stage of steadiness after 60 min (Fig. 6).

Effect of amount of adsorbent added

The effect of variation in the amount of adsorbent, CA@Fe_3O_4 (ranging from 5 to 30 mg) on the adsorption of CIP drug (10-50 ppm) using fixed volume of adsorbate solution (10 mL) and specific conditions, demonstrated that the removal efficiency

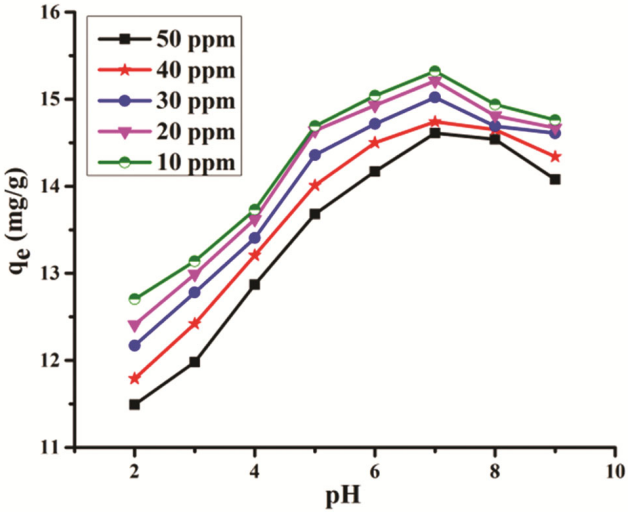

Fig. 5 — Effect of pH of solution on adsorption capacity (q_e) of citric acid functionalized magnetite nanoparticles (CA@Fe_3O_4) at various concentration of solution

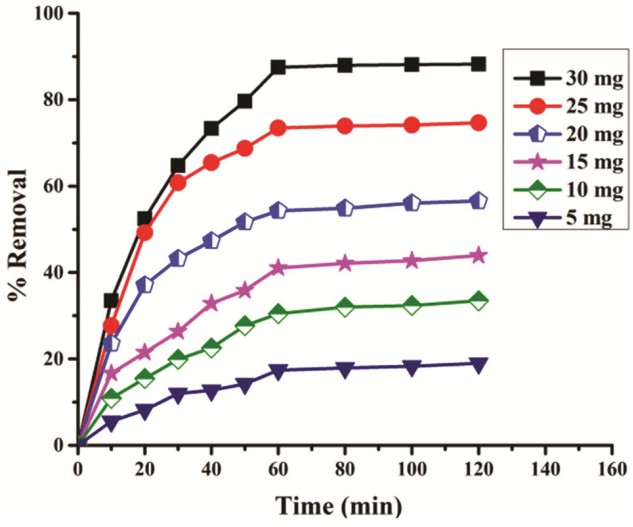

Fig. 6 — Effect on time on percentage removal of drug from aqueous solution using different amount of adsorbent in milligrams (05mg to 30 mg)

Table 3 — Isotherm Constants

Langmuir				Freundlich			Temkin		
R^2	q_m	K_L	R_L	R^2	n	K_F	R^2	A	B
0.9975	20.65 mg/g	0.64	0.301	0.8338	4.885	2.69	0.85683	14.775	3.204 J/mol

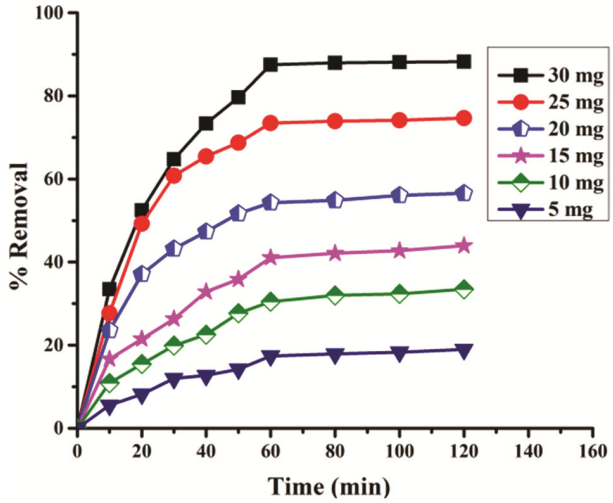

Fig. 7 — Effect of amount of adsorbent added on percentage removal of drug

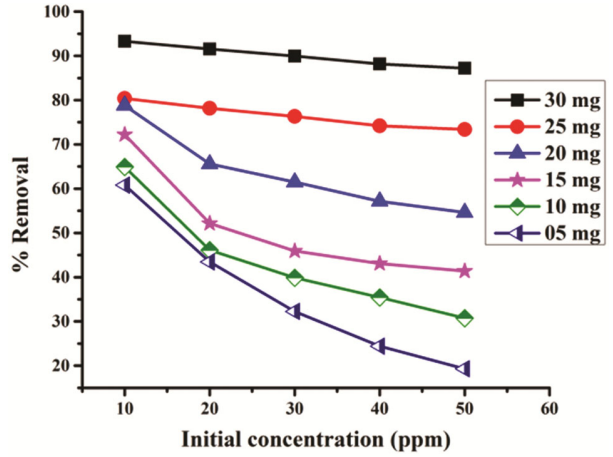

Fig. 8 — Effect of initial concentration of drug solution on percentage removal of drug using variable amount of adsorbent (05 mg to 30 mg)

gets increased with an increase in the amount of CA@Fe_3O_4 magnetite nanoparticles (Fig. 7). For instance, an increase in removal percentage of CIP drug was observed with the increase in the amount of CA@Fe_3O_4 magnetic nanoparticles.

Effect of initial concentration of drug solution

Drug solution of variable concentrations (10 to 50 ppm) was prepared to investigate the impact of initial concentration of these solutions on percentage removal using fixed amount of citric acid coated magnetite nanoparticles at optimum conditions. The

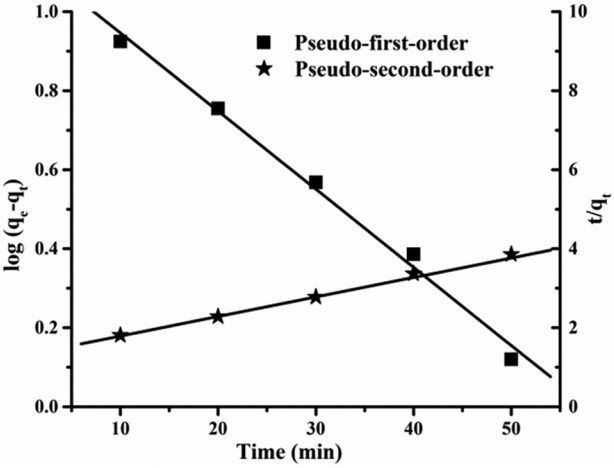

Fig. 9 — Kinetics model of adsorption study

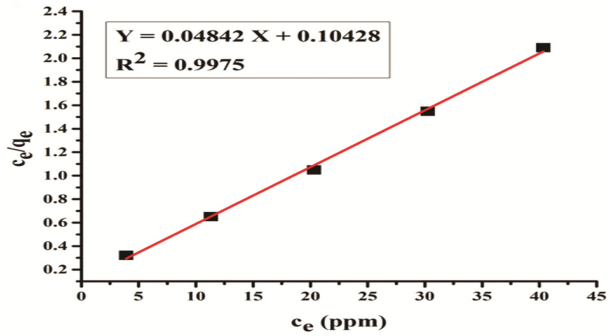

Fig. 10 — Langmuir isotherm model

fixed amount of citric acid coated magnetite nanoparticles provides static number of adsorption situates which results diminution in the percentage removal efficiency on increasing initial concentration of adsorbate solutions (Fig. 8).

Adsorption kinetic and isotherm study

The influence of contact time on adsorption behavior of CIP drug on the surface of citric acid coated magnetite nanoparticles illustrated that the equilibrium point was attained after 60 min for citric acid coated magnetite nanoparticles. The isotherm and kinetic studies[33] were carried out to observe the interactions and reaction rate of the adsorption process (Table 3). The results depicted that kinetics study follows pseudo-second-order model (Fig. 9) with good correlation coefficients (0.99951) while adsorption isotherm fitted better with Langmuir model with high correlation coefficients (Fig. 10) and

Table 4 — Zone of Inhibition.

Compounds	Diameter of Zone of Inhibition (mm)[a]			
	Gram Positive Bacteria		Gram Negative Bacteria	
	Bacillus subtilis	*Staphylococcus aureus*	*Pseudomonas aeruginosa*	*Escherichia coli*
CIP	32	26	28	26
CIP@CA@Fe_3O_4	35	28	29	28

[a]Values = included diameter of well

calculated maximum adsorption capacity was 20.65 mg/g. The kinetic study also revealed about the chemisorption of CIP drug over the surface of CA-@Fe_3O_4 nanoparticles and suggested that the adsorption capacity was related to the active sites of adsorbent[34].

Antibacterial activity of CIP@CA@Fe_3O_4

The ciprofloxacin drug loaded citric acid coated magnetite nanoparticles (CIP@CA@Fe_3O_4) were employed to check their antibacterial behavior. The results depicted that these loaded nanoparticles display greater antibacterial activity than standard drug against the similar bacterial strains (Table 4). Therefore the zone of inhibition is found to be greater for CIP@CA@Fe_3O_4.

Conclusion

The present study reported the synthesis and characterization of bare magnetite nanoparticles (Fe_3O_4) and citric acid coated magnetite nanoparticles (CA@Fe_3O_4). The adsorption of pollutants from aqueous solutions plays a considerable role. For this, the CA@Fe_3O_4 nanoparticles were used as an adsorbent for the adsorption of CIP drug from aqueous solution. The adsorption study suggested that CA@Fe_3O_4 nanoparticles depicted a good adsorption capacity for CIP drug due to the introduction of additional functional groups of citric acid and removed approximately 87.58% of CIP drug from aqueous solution for 30 mg of adsorbent. Adsorption isotherm was found to be dependent on Langmuir isotherm while kinetics fit well with pseudo-second-order reaction, suggesting that the adsorption process is a chemisorption process. Thus, these results demonstrated that CA@Fe_3O_4 nanoparticles could be used as an efficient and effective adsorbent for the adsorption of CIP drug from aqueous solution. Additionally, these drug loaded citric acid modified magnetite nanoparticles display remarkable antibacterial activities.

Acknowledgement

Co-authors, ArtiJangra, Jaiveer Singh, Jai Kumar and Keerti Rani, are highly thankful to Kurukshetra University, Kurukshetra, providing research facilities. The authors acknowledge UGC, New Delhi, India, for providing financial assistance in the form of a Junior Research Fellowship.

Conflict of interest

All authors declare no conflict of interest.

References

1 Xu X, He J, Li Y, Fang Z & Xu S, Adsorption and Transport of Ciprofloxacin in Quartz Sand at Different pH and Ionic Strength. *Open J Soil Sci*, 4 (2014) 407.
2 Ferrero F, Adsorption of Methylene Blue on magnesium silicate: Kinetics, equilibria and comparison with other adsorbents. *J Environ Sci*, 22 (2010) 467.
3 Chang SH, Wang KS, Li HC, Wey MY & Chou JD, Enhancement of Rhodamine B removal by low-cost fly ash sorption with Fenton pre-oxidation. *J Hazard Mater*, 172 (2009) 1131.
4 Jain R, Mathur M, Sikarwar S & Mittal A, Removal of the hazardous dye rhodamine B through photocatalytic and adsorption treatments. *J Environ Manage*, 85 (2007) 956.
5 Li Z, Hong H, Liao L, Ackley CJ, Schulz LA, MacDonald RA, Amanda L Mihelich AL & Emard SM, A mechanistic study of ciprofloxacin removal by kaolinite. *Colloids Surf B Biointerfaces*, 88 (2011) 339.
6 Jiang WT, Chang PH, Wang YS, Tsai Y, Jean JS, Li Z & Krukowski K, Removal of ciprofloxacin from water by birnessite. *J Hazard Mater*, 250–251 (2013) 362.
7 Rakshit S, Sarkar D, Elzinga EJ, Punamiya P & Datta R, Mechanisms of ciprofloxacin removal by nano-sized magnetite. *J Hazard Mater*, 246–247 (2013) 221.
8 Wang F, Yang B, Wang H, Song Q, Tan F & Cao Y, Removal of ciprofloxacin from aqueous solution by a magnetic chitosan grafted graphene oxide composite. *J Mol Liq*, 222 (2016) 188.
9 Wang YX, Ngo HH & Guo WS, Preparation of a specific bamboo based activated carbon and its application for ciprofloxacin removal. *Sci Total Environ*, 533 (2015) 32.
10 Khoshnamvand N, Ahmadi S & Mostafapour FK, Kinetic and Isotherm Studies on Ciprofloxacin an Adsorption using Magnesium Oxide Nanopartices Water and Wastewater Treatment View project Kinetic and Isotherm Studies on Ciprofloxacin an Adsorption using Magnesium Oxide Nanopartices. *J Appl Pharm Sci*, 7 (2017) 79.
11 Li J, Yu G, Pan L, Li C, You F, Xie S, Wang Y, Ma J & Shang X, Study of ciprofloxacin removal by biochar obtained from used tea leaves. *J Environ Sci (China)*, 73 (2018) 20.
12 Liu Z, Ding J & Xue J, A new family of biocompatible and stable magnetic nanoparticles: Silica cross-linked pluronic F127 micelles loaded with iron oxides. *New J Chem*, 33 (2009) 88.

13 Petri-Fink A, Chastellain M, Juillerat-Jeanneret L, Ferrari A & Hofmann H, Development of functionalized superparamagnetic iron oxide nanoparticles for interaction with human cancer cells. *Biomaterials*, 26 (2005) 2685.

14 Sahoo Y, Goodarzi A, Swihart MT, Ohulchanskyy TY, Kaur N, Furlani EP & Prasad PN, Aqueous Ferrofluid of Magnetite Nanoparticles: Fluorescence Labeling and Magnetophoretic Control. *J Phys Chem B*, 109 (2005) 3879.

15 Nayak S, Lee H, Chmielewski J & Lyon LA, Folate-mediated cell targeting and cytotoxicity using thermoresponsive microgels. *J Am Chem Soc*, 126 (2004) 10258.

16 Jangra A, Singh J, Khanna R, Kumar P, Kumar S & Kumar R, Comparative studies of dye removal efficiency of surface functionalized nanoparticles with other adsorbents: Isotherm and kinetic study. *Asian J Chem*, 33 (2021) 3031.

17 Singh D, Gautam RK, Kumar R, Shukla BK, Shankar V & Krishna V, Citric acid coated magnetic nanoparticles: Synthesis, characterization and application in removal of Cd(II) ions from aqueous solution. *J Water Process Eng*, 4 (2014) 233.

18 Langmuir I, The adsorption of gases on plane surfaces of glass, mica and platinum. *J Am Chem Soc*, 40 (1918) 1361.

19 Al-Trawneh SA, Jiries AG, Alshahateet SF & Sagadevan S, Phenol removal from aqueous solution using synthetic V-shaped organic adsorbent: Kinetics, isotherm, and thermodynamics studies. *Chem Phys Lett*, 781 (2021) 138959.

20 Freundlich H, Über die Adsorption in Lösungen. *Zeitschrift Für Phys Chemie*, 57U (1907) 385.

21 İsmail O & Kocabay ÖG, Absorption and adsorption studies of polyacrylamide/sodium alginate hydrogels. *Colloid Polym Sci*, 299 (2021) 783.

22 Temkin MJ & Pyzhev V, Recent modifications to Langmuir isotherms. Acta Physiochim URSS, 12 (1940) 217.

23 Elemile OO, Akpor BO, Ibitogbe EM, Afolabi YT & Ajani DO, Adsorption isotherm and kinetics for the removal of nitrate from wastewater using chicken feather fiber. *Cogent Eng*, 9 (2022)

24 Lagergren S, Zur Theorie der sogenannten Adsorption gelostn. *Zeitschrift für Chemie*, 2 (1898) 15.

25 Ghibate R, Senhaji O & Taouil R, Kinetic and thermodynamic approaches on Rhodamine B adsorption onto pomegranate peel. *Case Stud Chem Environ Eng*, 3 (2021) 100078.

26 Ho YS & McKay G, Pseudo-second order model for sorption processes. *Process Biochem*, 34 (1999) 451.

27 Singh J, Jangra A, Rani K, Kumar P, Kumar S & Kumar R, Kinetic and Thermal Studies of Adsorption of Allura Red Dye by Surface Functionalized Magnetite Nanoparticles. *Asian J Chem*, 33 (2021) 2675.

28 Kumar J, Kumar P, Kumar S, Langyan R & Kumar R, Template directed synthesis and characterization of macrocyclic complexes : *In-silico* docking and antimicrobial studies. *Rasayan J Chem*, 14 (2021) 2567.

29 Lan Q, Liu C, Yang F, Liu S, Xu J & Sun D, Synthesis of bilayer oleic acid-coated Fe3O4 nanoparticles and their application in pH-responsive Pickering emulsions. *J Colloid Interface Sci*, 310 (2007) 260.

30 Goodarzi A, Sahoo Y, Swihart MT & Prasad PN, Aqueous ferrofluid of citric acid coated magnetite particles. *Mat Res Soc Symp Proc*, 789 (2003) 129.

31 Cao E, Duan W, Wang A & Zheng Y, Oriented growth of poly(m-phenylenediamine) on Calotropis gigantea fiber for rapid adsorption of ciprofloxacin. *Chemosphere*, 171 (2017) 223.

32 Zhuang Y, Yu F, Ma J & Chen J, Adsorption of ciprofloxacin onto graphene–soy protein biocomposites. *New J Chem*, 39 (2015) 3333.

33 Ammar F, Rachid C, Amel A & Naima A, Kinetics and isotherms modeling of methylene blue adsorption by black carbon using the shells of apricot kernels. *Indian J Chem Technol*, 28 (2021) 412.

34 Ji L, Chen W, Duan L & Zhu D, Mechanisms for strong adsorption of tetracycline to carbon nanotubes: A comparative study using activated carbon and graphite as adsorbents. *Environ Sci Technol*, 43 (2009) 2322.